uc3m | Universidad Carlos III de Madrid

BACHELOR'S THESIS

Degree in Aerospace Engineering

Autogyro C-30 Fuselage Finite Element Model Analysis

Enrique Labiano Laserna

Supervisor

José Díaz Álvarez

February 2019

Abstract

The main objective of this paper is to design and analyze the autogyro C-30 fuselage structure. The autogyro, considered as a hybrid between an airplane and a helicopter, is one the most important milestone in aircraft aviation. It was invented by Juan De la Cierva and became the first rotary wing aircraft that achieved success. In fact, this kind of rotorcraft will have a lot of influence on how the helicopter operates nowadays.

The project will be divided into several parts. Firstly, all the information and drawings of the fuselage structure will be gathered and analyzed. After that, the fuselage structure will be modeled in a finite element software, called *Abaqus*. Secondly, all parts that composed the autogyro will be determined and their weights will be estimated taking into account the MTOW of the aircraft. According to the regulations established in the British Civil Airworthiness Requirements (BCAR), loads will be introduced in the model simulating a symmetric pull-up maneuver. The scope of the study will involve a stress analysis and finally, a modal analysis in order to determine the natural frequencies of the structure.

Finally, a socio-economic impact of designing an autogyro will be presented together with a rough budget of manufacturing the fuselage structure of the autogyro C-30.

Keywords: Autogyro C-30, fuselage structure, FEM analysis, modal analysis

Acknowledgements

First of all, I would like to thank my parents and my brothers who have helped me from the beginning. You know better than anyone the bad moments I have passed during the degree. So, just wanted to let you know thanks for being always with me and keeping your faith in me, your love and support has made this possible.

Besides this, thanks to José Díaz for all your help and patience with me. Thanks for sharing your time and for teaching me during these years. It has been a pleasure to be your pupil. Also, thanks to Juan Manuel Arco for providing me all the documents related with the autogyro and transmit me all your passion about aircraft.

I would like to thank all my classmates Cristóbal, Juan, Alberto, Mercedes, Diego and Elena, these four years would not have been the same without you.

Finally, I would like to mention all my friends from school. Thanks for being patient with me and for understanding me when I couldn't meet up with you due to the heavy workload at university. From this point on, I promise to be much more time with you.

Contents

List of Figures

List of Tables

List of abbreviations

Acronym	Stands for
AMC	Acceptable Means of Compliance
BCAR	British Civil Airworthiness Requirements
BWG	Birmingham Wire Gauge
CAA	Civil Aviation Authority
CS	Certification Specifications
EASA	European Aviation Safety Agency
FEA	Finite Element Analysis
FEM	Finite Element Method
MAESAL	Maestranza Aérea de Albacete
MTOW	Maximum Takeoff Weight
OEW	Operational Empty Weight
RAF	Royal Air Force
UAV	Unmanned aerial vehicles
VLA	Very Light Aeroplanes
VLR	Very Light Rotorcraft

1 Introduction

This section aims to make an approach to the reader about autogyros. First of all, a description of the problem and the main objectives of the project are presented. Then, the beginnings of the rotary wing aircraft until the invention of the autogyro are introduced. Finally, the main operating principle of this technology is described.

1.1 Statement of the problem

Juan de la Cierva Association wants to commemorate the centenary of the world's first flight of the autogyro. For this reason, they are leading a project called "Juanito C-30" with the purpose of making a replica of the autogyro C-30. Its main goal is to manufacture a new C-30 model as close as possible to the original one. In fact, most patents and principles of the original autogyro will be maintained, and just a few modifications and improvements will be introduced in order to increase safety. This model will be used to perform sports exhibitions and, in this way, promoting one of the most important Spanish aviation figures.

Figure 1: Autogyro C-30 model [1]

The C-30 has a maximum takeoff weight of 850 kg. It is propelled by a fixed-pitch propeller of 2.1 m of diameter connected to a Civet I engine of 140 HP reaching speeds up to 200 km/h. The lift was produced by a 11.3 m rotor diameter composed of three blades rotating at almost 200 rpm [2].

1.2 Scope of the project

The main objective of this project is to design and analyse the fuselage structure of the autogyro C-30 made by the Cierva Autogiro Company. First of all, a research work was performed in order to obtain the drawings of the structure. Documentation and notes provided by the *Juan de la Cierva Association* and from the Maestranza Aérea de Albacete (MAESAL) will be used.

After that, the fuselage will be defined and introduced in a finite element software called *Abaqus*. Additionally, several components will be added to the fuselage, like the landing gear, the engine mount and the pylon structure of the rotor, mainly because they will produce loads that affect the fuselage. Notice that these additional elements will be simplified structures.

A structural stress analysis will be performed when the system is subjected to loads that simulate a symmetric pull-up maneuver. However, since there is no information about the flight loads, a rough estimation of the weights and loads expected in service will be made. All strength and deformation requirements will be made in compliance with the British Civil Airworthiness Requirements (BCAR): Section T Light Gyroplanes. The limit manoeuvring load factor and safety factor will be determined by this normative in order to guarantee its functionality. Besides this, the maximum safety factor that the structure can support in a symmetric pull up before breaks will be calculated.

Finally, a modal analysis of the structure will be performed in order to calculate the natural frequencies and the mode shapes of the system. This will allow knowing which are the most dangerous frequencies that could produce the failure of the structure.

1.3 First approach to autogyros

At the beginning of the 20^{th} century with all advances in aerodynamics, structures and propulsion, the dream of flying became a reality when the Wright brothers designed the world's first practical airplane. In 1905, the first powered, controlled and sustained flight was performed with the Flyer III [3]. From this point on, continuous and huge improvements were achieved in the aeronautical world. However, most aircraft designed during this period will have problems and accidents caused, among others, by engine failures that would produce the aircraft enter in stall.

Juan de la Cierva, an aerospace engineer, realised that some innovations had to be introduced in order to increase aviation safety. Nevertheless, he will focus on the development of rotary-wing aircraft instead of the fixed-wing concept, in particular, on the autorotation principle. His main objective will be to develop an aircraft in which the lift does not depend on the propulsion system, and therefore, avoid accidents produced by engine failures.

The concept of flying with rotary wings comes from many years ago, starting with Leonardo da Vinci in the XV century. One of the ideas of da Vinci's flying machines was the aerial screw, in which the concept of lifting up a vehicle by spinning a rotary blade was introduced. Unfortunately, most of his drawings were never constructed due to the limit technology available at that time. But, it is evident that most of the models about designing a flying machine will be a source of inspiration for the next inventors [4].

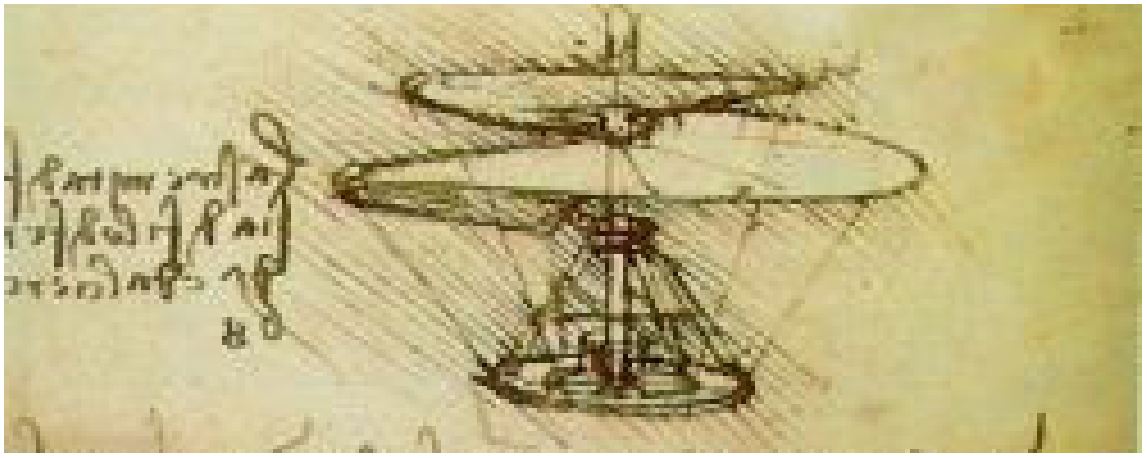

Figure 2: Helical air screw [4]

In the early 1900s, a lot of rotary-wing machines achieved somehow lift itself vertically from the ground, but they just achieved short jumps. All of them could not fly due to aerodynamic and mechanical problems, most of them related to the control, stability and the lack of a powerful engine. With all these problems in attaining vertical flight, the possibility of flying with a rotary wing aircraft seemed to be remote until the invention of Juan de la Cierva.

However during the first autogyro protoypes, De la Cierva found the same problem as many rotary wing aircraft designers: the dissymetry of lift. This happened because the rotor blades were still rigid and therefore, when rotating, an unbalanced rolling moment was generated, producing the aircraft to tip over before leaving the ground. De la Cierva solved this problem with the design of an articulated rotor, in which the blades are attached to flapping hinges. In this way, blades are able to rotate and to change its angle of attack in order to produce the same amount of lift on both side of the main rotor disc [5]. With this invention, De la Cierva found the solution to the lift asymmetry problem and demonstrated that a rotary-wing could produce lift by itself without the need of an engine.

In 1923, De la Cierva invented a new type aircraft: the autogyro. The articulated rotor was successfully introduced in the prototype C-4, achieving the first successful flight of a rotary-wing aircraft. From this point on, a lot of companies were interested in their patents and thanks to these economic resources, De la Cierva will continue improving the development of the autogyro [5].

Finally, in 1933 Juan de la Cierva would finish his development of the rotary-wing with the design of the autogyro C-30, including improvements that would increase the control of the aircraft. This model, where the lift was produced by non-powered rotating blades, represented one of the greatest advances in the aviation world.

Figure 3: Autogyro C-30 [6]

1.4 How the autogyro works

An autogyro is a rotary wing aircraft that can be considered as a combination of a fixed-wing airplane and a helicopter. The forward thrust is provided by an engine-driven propeller and the lift is generated by an unpowered rotor which is free to rotate. One of the main differences with the helicopter is the rotor system. In the helicopter, both thrust and lift are produced by a powered rotor connected to an engine. This provides the helicopter the ability to take-off and landing vertically and to remain stopped in the air (hover). Unlike the helicopter, the autogyro cannot hover, and it is not able to take-off vertically. However, the autogyro can fly at very low speed maintaining a sustained flight without entering in stall.

As it has been mentioned before, the key of de la Cierva's stable aircraft was the introduction of a flapping hinge (figure 4). This mechanism changes the angle of attack of the rotor blades allowing to equalize the lift between the advancing and retreating blades and to compensate for the dissymmetry of lift.

When the aircraft is moving forward by the action of the propeller, the stream of air moving up through the rotor will produce the blades to rotate and generate lift (see figure 5). This aerodynamic phenomenon is called autorotation [7].

In case of an engine failure, the aircraft will start to descent slowly, with the blades self-rotating due to the autorotation principle. Indeed, more air will pass through the blades increasing the rotation and thus, the lift. The aircraft will not enter in stall, and a controlled and smooth landing will be performed. In fact, the pilot would have to follow the same procedure as in normal conditions, and where the autogyro will settle to the ground more slowly than a parachute does. The autorotation principle will make the autogyro to be the safest aircraft in the world [7].

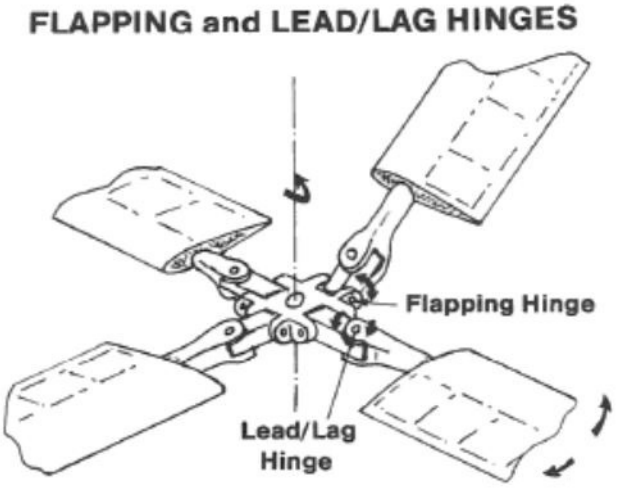

Figure 4: Flapping hinge [8]

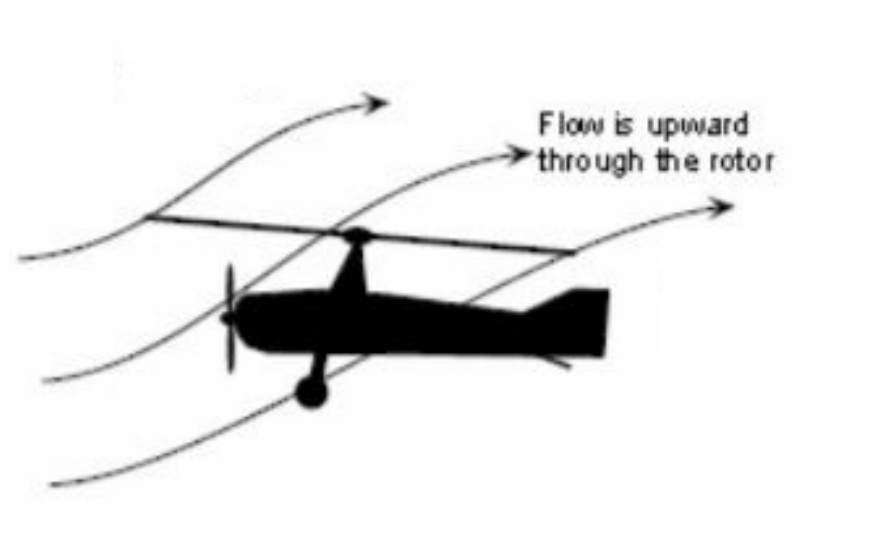

Figure 5: Principle of operation [9]

2 State of the art

The autogyro, one of the greatest achievement in aviation, was the beginning of a new era in the aerospace industry. Juan de la Cierva proved to the world that it was possible to fly with a rotary wing aircraft with no engine power. At the same time, thanks to the contribution of the autogyro, the first successes with helicopters started to appear. However, in 1936, Juan de la Cierva died in an aircraft accident, establishing a turning point in the development of the autogyro. The autogyro will be used for surveillance and reconnaissance roles at the World War II, but few years later, the autogyro would be almost ceased to be marketed [10].

The helicopter will be further developed due to its advantages over the autogyro. Its great manoeuvrability, its ability to hover and to perform vertical take-off, made the helicopter a more attractive option for most companies. From this point on, the helicopter will become more and more successful, being one of the most important means of transport nowadays. For this reason, there is not considerable information or projects related to the autogyro.

Regarding the autogyro C-30, there exists a handbook made by the Royal Air Force (RAF) related to the construction of an original C-30. This handbook, called *The Rota Gyroplane*, is divided into three independent volumes [11]. In the Volumen I, a general description of the autogyro and its main components are presented. Besides this, special flying notes such as starting up the engine or the procedure to perform take-offs and landings are described. In the Volume II, drawings of the C-30 fuselage structure are shown. In addition, a maintenance schedule in order to maintain the aircraft ready for flight is given. In the last volume, a list of spare parts is described together with the instructions for repair.

Furthermore, there are documents and information from a C-30 replica construction made by the MAESAL in 1998. This model, called "C-30 MZA" was built in collaboration with the RAF museum that provided parts from an original C-30 made by the Cierva Autogyro Company. Nevertheless, after several flights, the aircraft had an accident and was handed over the Museo del Aire [12]. Nowadays, this autogyro model is declared as a property of cultural interest and cannot be flown. From this replica construction, another handbook can be extracted [2], which is very similar to the *Rota Gyroplane*. The main difference is that exists information about the Siemens-Halke SH 14 engine, implemented as a modification with respect to the original C-30.

Besides this, an investigation into the principal characteristics of the autogyro C-30 is presented in [6]. This paper focuses on the performance and aerodynamic characteristics of the rotating blades. Another relevant study is given in [13], where a detailed description of the autogyro C-30 is presented. This document provided a good insight on how components are distributed along the aircraft. Moreover, general characteristics and performances of the aircraft are given.

Currently, there is not too much interest in develop autogyros for commercial or military purposes, mainly because of most of the missions and uses can be performed either by an airplane or a helicopter. In fact, a lot of autogyro designs are only used for sports exhibition. However, there exist some companies that are still trying to develop the autogyro concept:

- **Skyworks Global**: Formerly known as Groen Brothers aviation, it is considered as one of the global leaders in the science and technology of autogyros. This American company focuses on the development of high-performance autogyros by introducing some of the helicopter concepts with the main objective of making air transport cheaper and safer. One of its future design is the "ScoutHawk". This model, based on the principle of the autorotative flight, presents the capability of performing vertical take-offs and landings, safety and an operational cost much lower than modern helicopters. By using advanced technologies and sciences, Skyworks Global want to create a new revolutionary era in the development of the autogyro [14].
- **AutoGyro GmbH** : this German company is one of the most important autogyro manufacturers in Europe. It stands out for making the first electric autogyro, named as "e-Cavalon". With the help of Bosch, that provided and implemented an electric engine, this model has successfully completed all ground and flight tests. However, it continues under development, in order to increase the useful life of the battery and therefore the range of the autogyro [15].

Figure 6: E-cavalon model [15]

3 Regulatory framework

The European Aviation Safety Agency (EASA) is one of the most important regulators in the air transport industry. It includes all members countries of the European Union. Among other tasks, it is responsible for elaborating rules and certifications imposed on both aircraft manufacturers and operators in order to ensure the highest level of safety. Most airworthiness requirements and standards issued are focused on general aviation like helicopters or airplanes. Nevertheless, there are not any Certification Specifications (CS) for autogyros [16].

The replica construction of the autogyro C-30 will be an amateur design. According to the *Regulation (EC) [216/2008]Article 4, Annex II*, all amateur designs remain under the legal framework of the national civil aviation authorities. However, only standards for ultralight autogyros exist, where the maximum take-off weight (MTOW) is lower than 560 kg [17]. Therefore, since the MTOW of the autogyro C-30 is 850 kg, these regulations should not be applied. One possible solution might be to apply some of the regulations issued for very light aeroplanes (*CS-VLA*) or for light rotorcraft (*CS-VLR*) as the autogyro can be considered as a combination of both. Other solution would be to apply regulations for ultralight autogyro even though the C-30 weight is greater than the required.

For the sake of simplicity, in this paper safety standards for ultralight autogyros will be applied. It must be noted that ultralight aircraft class are not covered by EASA and remain under the legal framework of the national aviation institutions. This is the case of the Civil Aviation Authority (CAA) which is responsible for regulating and oversees all airworthiness requirements and operational rules within the United Kingdom [18].

One of the most common worldwide standard for light autogyros is the Section T of the British Civil Airworthiness Requirements (BCAR). It comprises all certifications and standards needed in order to obtain permits and approvals to fly. This document is composed of two parts. The first part covers all requirements whereas the second one, called Acceptable Means of Compliance (AMC), acceptable methods of interpretation of requirements are explained [19].

As the scope of this study is a structural stress analysis, the following safety standards for light autogyro have been considered in accordance with [19]:

- **Loads**
  - *Strength requirements are specified in terms of limit loads and ultimate loads.*
  - *Loads must be placed so as to represent real conditions or a conservative approximation to them.*

- **Factor of safety**
  - *A safety factor of 1.5 must be used.*
- **Strength and deformation**
  - *The structure must support limit loads and ultimate loads without permanent deformation.*
- **Limit maneuvering load factor**
  - *A limit maneuvering load factor of 3.5 must be used.*
- **Engine torque**
  - *Engine mounting must support the limit torque achieved when operating at maximum continuous power together with the loads expected in service.*
  - *A factor of 1.33 must be applied to the torque in a seven-stroke engine.*

4 Methodology

This section will present a brief introduction to the Finite Element Method (FEM). Then, a description of the model, including the geometry and design specifications will be introduced. Since the complete drawings of the autogyro do not exist, several assumptions will be taken when designing some of the parts in such a way that the model resembles as closely as possible to the original one. Finally, the weight of each of the elements that comprise the model and the corresponding loads will be estimated.

4.1 Introduction to FEM

As previously explained, a simplified model of the fuselage structure will be implemented in *Abaqus*. This software uses a finite element method to solve complex numerical computations. A finite element analysis (FEA) is used to solve boundary value problems, which are problems governed by differential equations defined throughout a region and with initial conditions. Most companies will use these kinds of programs to simulate virtual models. This will allow the companies to save money and time as the best option would be selected without performing the manufacture of real and expensive models.

Basically, a finite element analysis is used to obtain an approximate solution to most real world problems in a fast way. From the user perspective, this kind of analysis will consist on several steps. Firstly, define the problem and create a model by specifying the geometry and material properties. Then, a discretization process is carried out in order to have a finite number of elements and nodes. Note that *Abaqus Student Edition* is restricted to 1000 nodes. After that, a type of analysis is selected and the loads and boundary conditions are applied. The computer will establish relationships between forces and displacements in each of the elements and nodes. Then, all these pieces are linking together by an assembly process giving a large system of equations. The program will solve these complex equations and the behaviour of the system will be depicted in the post-processing module [20].

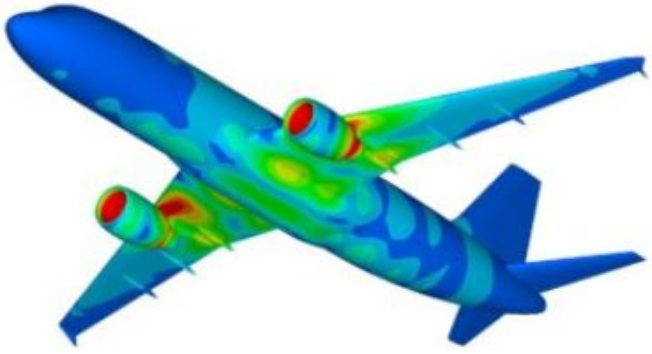

Figure 7: Finite Element Analysis of an aircraft [21]

4.2 Fuselage design process

In order to model the fuselage structure, the drawing shown in Appendix A has been used [22], where all structure dimensions are depicted. Actually, this is one of the few drawings of the C-30 that exists because the rest of them are lost. So, for the other elements pictures, notes and sketches will be used for their design.

As it can be visualized in Appendix B, the structure is composed of 63 types of tubes. However, the dimensions of the tubes will be defined in terms of the outside diameter and the gauge. For this reason, the chart found in [23] is used to calculate the wall thickness based on the gauge given. The nominal tube dimensions found in this table are based on the Birmingham Wire Gauge system (BWG), which is a standard used for describing the thickness of steel tubes. Once the tube sizes are calculated (see Appendix C), the model in *Abaqus* is created.

The entire structure is made up of steel tubes, which are treated in *Abaqus* as thin-walled beams (wall thickness is much smaller compared to its length) with a closed section. Therefore, the whole fuselage will be designed as a structure composed of beams, which are elements able to support axial, bending, shear and torsional loads. In *Abaqus*, beam elements are represented in a 3D modeling space as 1D line element (wire) joint by means of nodes.

The first step is to make a sketch of the structure. For this purpose, a 3D wire element is selected as base feature, in such a way that the fuselage is designed as a wire structure (see figure 8). Note that in *Abaqus*, only beam sections can be applied to wire regions. Next step is to specify what kind of joints exist between the beam elements. As most steel structures, fixed connections are used. The nodes between the beam elements are treated as welds, so that is, all beams are fused together at the joints. Welded connections restrain both translation and rotation but allow transfer of moments between members.

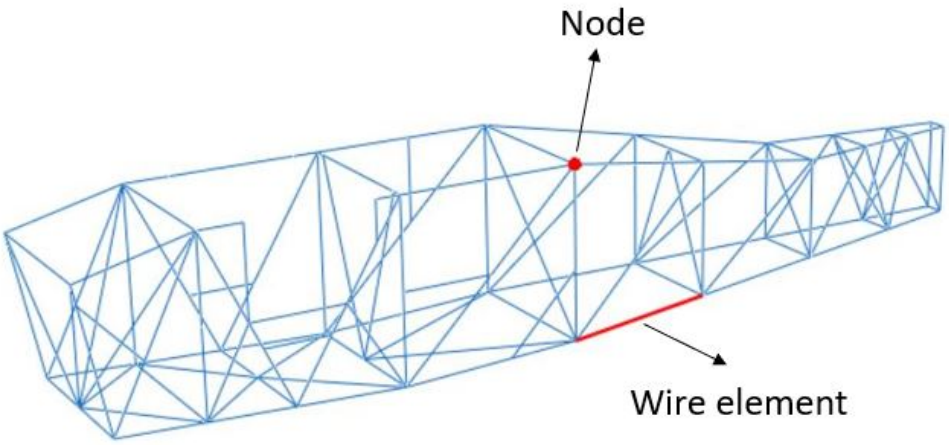

Figure 8: Fuselage sketch

The whole of the material used in the model is the AISI 4130 Alloy Steel. This material shows good weldability and machinability. It also presents high corrosion resistance and good fatigue and tensile strength. This will make the 4130 steel be one of the most common option for constructing airframe structures in the aerospace industry. Note that the material properties are assumed to be linear, and therefore time-dependent material effects will be neglected. Its properties are shown below [24]:

Property	**Value**
Density, ρ	7850 kg/m^3
Young's Modulus, E	205 GPa
Poison's Ratio, υ	0.29
Ultimate strength, σ_y	435 MPa

Table 2: Material Properties

Using this material, the geometries of the cross-sections of the beams are created. The cross-sectional profiles are introduced as tubes, defining the corresponding outside diameter and wall thickness. Each of the beams sections are assigned to the corresponding wires, obtaining the following model :

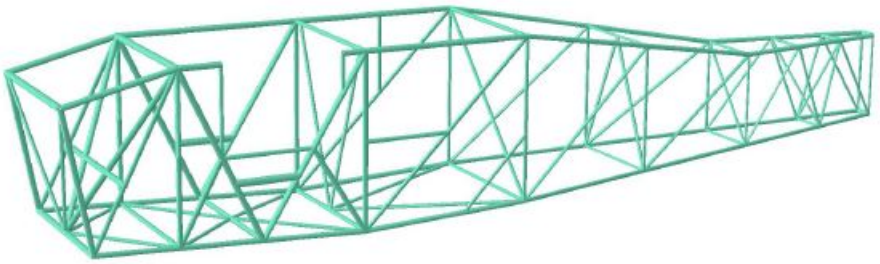

Figure 9: Fuselage structure model

4.2.1 Final model

As previously stated, it has been necessary to introduce more regions apart from the fuselage structure in order to apply a particular set of loads. In *Abaqus*, physical points are needed in order to apply loads. The additional regions can be appreciated in figures 10, 11 and 12 where the engine mounting, landing gear and pylon structure of the rotor have been designed together with the fuselage structure.

The dimensions of the engine mounting structure and its tubes were obtained from the documentation. However, there are no drawings for the rest of additional elements to work from. The solution was to make scale drawings of both landing gear and pylon structure based on pictures and notes. In this way, a simplified version

of the autogyro is created by estimating the dimensions and lengths of the tubes that comprise these extra elements. Nevertheless, the inner diameter could not be estimated, and thus, the geometry of these tubes cannot be designed. For this reason, the following procedure has been carried out in order to estimate the inside diameter.

Firstly, an approximated design or sketch of each of the structures was performed in order to obtain the lengths of the tubes. Then, the weight of each of the structures is estimated as explained in *Section* 4.4.3 . With this data, it is possible to compute the inner radius of the tubes as described hereunder.

The material used is the same as the fuselage structure, therefore, the value of the density is the one depicts in table 2. The area can be obtained from the density equation as :

$$\rho = \frac{m}{V} = \frac{m}{AL} \qquad \rightarrow \qquad A = \frac{m}{\rho L} \tag{1}$$

where V is the volume represented as area (A) times length (L).

Besides this, each of the structures (landing gear and pylon structure) is formed by several members or tubes. The weights of each of these tubes, denoted by the sub-index i, can be estimated as :

$$m_i = \frac{m_t L_i}{L_t} \tag{2}$$

where m_i and L_i represent the mass and length of one tube, respectively, and m_t and L_t refer to the total weight and length of the structure studied, respectively. Note that m_t (estimated), L_i and L_t (obtained from a scale drawing), are known parameters.

Introducing equation 2 into equation 1, the cross-sectional area of a tube can be rewritten as :

$$A_i = \frac{m_i}{\rho L_i} = \frac{m_t}{\rho L_t} \tag{3}$$

In the same way, it can be computed as well as :

$$A = \pi \left(R^2 - r^2\right) \tag{4}$$

where R refers to the outside diameter and r to the inner diameter. Combining both equations 3 and 4 and solving for r, the resulting equation turn out to be :

$$r = \sqrt{R^2 - \frac{m_t}{\pi \rho L_t}} \tag{5}$$

Using equation 5, the inside diameter of the tubes are calculated. This procedure has been performed for both landing gear and pylon structure. It must be pointed out that all tubes belonging to the same structure have been assumed to be of the same type, and therefore, having the same inner and outside diameter. The resultant tubes dimensions can be visualized in Appendix C.

The final model can be appreciated in figures 10, 11 and 12. The engine mount, located in the front part, is joint to the fuselage by means of eight tubes, that are welded in the ends of the top and bottom longerons. The pylon structure consists of four struts welded to the four attachments points located at the front cockpit cabin. Finally, the main landing gear (both left and right) is made up of six tubes welded to different points along the four longerons on either sides. The tail landing gear consists of two tubes joint to the fuselage structure.

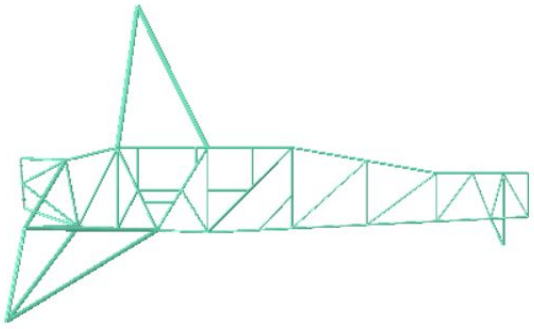

Figure 10: Lateral view

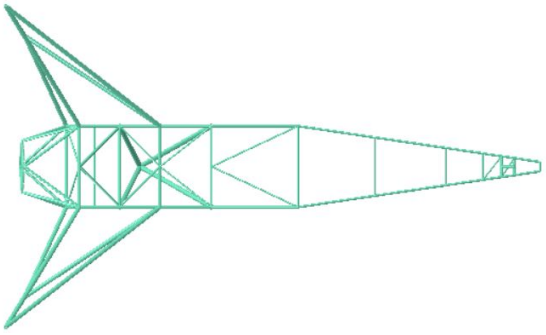

Figure 11: Top view

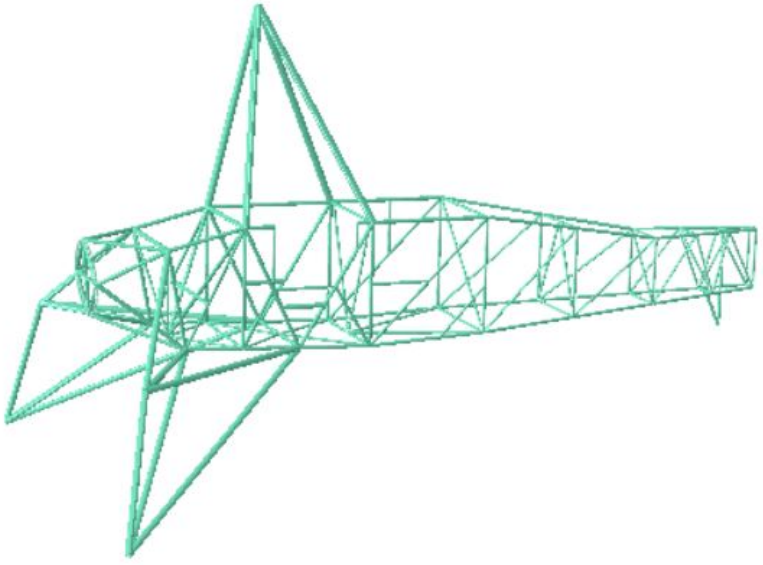

Figure 12: Autogyro C-30 simplified model

4.3 Components of the autogyro

Most of the loads are due to the weight of the components that comprise the autogyro. Therefore, the first step will be to determine the weight of all these substructures and elements. For this reason, a simplified and approximated description of the fuselage will be presented to the reader in order to clearly distinguish the main components. The principal regions of the fuselage structure or skeleton are depicted in figure 13. In this figure, the principal zones are highlighted for better understanding the distribution of the components.

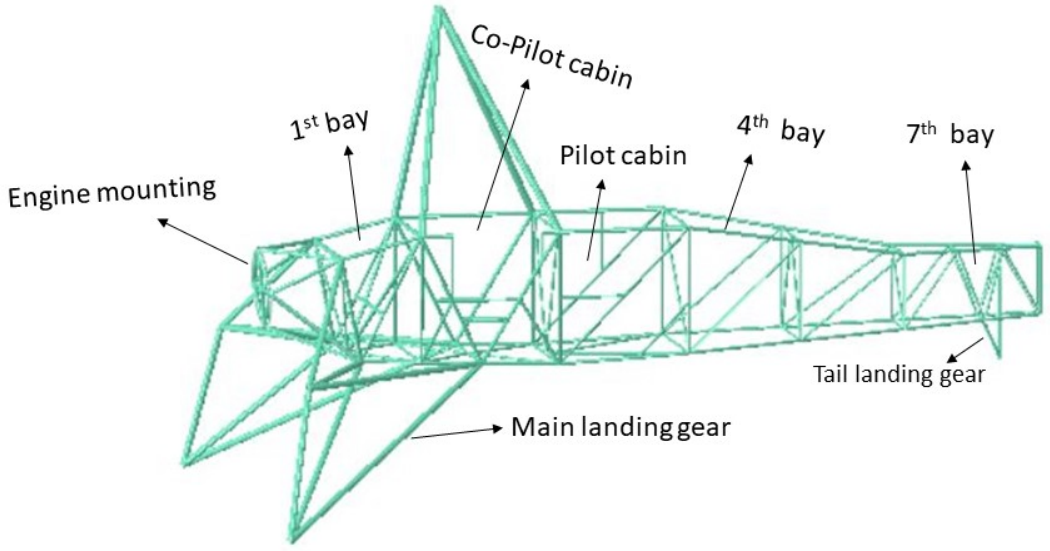

Figure 13: Main regions of the autogyro C-30

The real model of the autogyro C-30 has a fuselage made up with a semi-monocoque construction as it is shown in figure 14. This type of airframe construction is formed by a skeleton structure and a skin. The skin covers the fuselage structure and in a real flight, it transmits the aerodynamic loads into the longitudinal and transversal elements. In the longitudinal direction, stringers are placed acting as stiffeners and are attached to the formers (frames). Furthermore, four longerons are longitudinally placed in the fuselage skeleton carrying most of the axial loads. In the transversal direction, formers are used to maintain the shape of the fuselage and to prevent buckling [25]. It must be noted that in this paper only the the fuselage structure (skeleton) will be object of study assuming that supports all the loads and stresses.

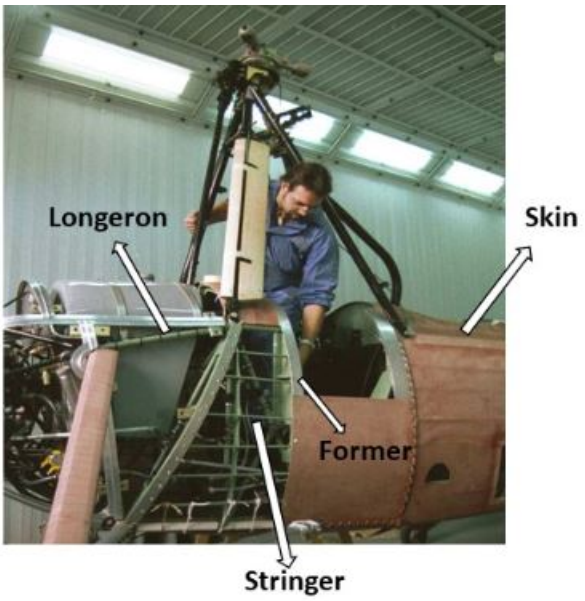

Figure 14: Semi-Monocoque fuselage

Now, a deep description of the fuselage structure is presented in order to locate the main parts that conforms it. Basically, the fuselage can be divided into three regions. The first one covers the engine mount and the first bay; the second one comprises both cockpits, and the last one the rear part of the fuselage [26].

The first region, so that is, from the engine mounting to the end of the first bay, is covered by an aluminium skin due to the high temperatures achieved by the engine. In the front part of the first bay or confinement, the mechanical starter and the clutch system are placed for starting the engine. Additionally, in the upper part, the fuel tank is mounted whereas the oil tank rests in the lower one.

Regarding the second region, the co-pilot and pilot cabin are accommodated together with the parachute type seats in the second and third bay, respectively. All devices and instruments are distributed within this region as well. Besides this, the pylon structure is welded to the fuselage at the four attachments points located on the top longerons of the front cockpit.

The third region covers from the fourth bay until the end. This zone is mainly cross-braced with steel tubing in order to reinforce the structure. At the rear portion, the horizontal and vertical stabilizers are installed and welded to the fuselage structure in the seventh and eighth bay respectively.

Notice that the second and third region are also composed of formers and stringers that run across the whole fuselage. These elements have been assumed to be made up with steel forming a framework over which a plywood skin is fabric-covered. Additionally, two opening cut-outs are performed in the skin to access the pilot and co-pilot cabin respectively.

4.4 Weight estimation

As stated before, there are no documents related to the weight of each of the elements that comprise the autogyro. For this reason, a weight estimation procedure has been carried out. Moreover, the worst scenario will be simulated assuming a full load case. Note that the words "mass" and "weight" are considered as equivalent in this paper.

According to a weight analysis performed in [6], the maximum takeoff weight (MTOW) of the autogyro is 850 kg and the tare or operational empty weight (OEW) is 572 kg. Using this information, all weights will be distributed in such a way that the maximum design aircraft weight is achieved.

First of all, the autogyro will be divided into three main weight groups in order to account for the total aircraft mass : Operational Empty Weight (OEW), Payload and Fuel-Oil. In this way, the maximum weight of the autogyro can be written as :

$$W_{MTOW} = W_{OEW} + W_{payload} + W_{fuel+oil} \tag{6}$$

4.4.1 Fuel and Oil

The fuel weight is computed from the tank capacity and the density of the jet fuel. The fuel is carried in a 24 gallon tank, so that is, 91 liters. The fuel density is assumed to be 0.82 kg/l. In this way, the maximum fuel weight is calculated as follows:

$$W_{fuel} = V_f \rho_f = 91 \cdot 0.82 = 75 \ kg \tag{7}$$

Although the fuel was provided entirely by gravity, an additional weight related to the fuel control system like the carburetor or the tank's own weight have been considered. Hence, the final value of the total fuel weight is estimated as :

$$\mathbf{W_{fuel} = 80 \ kg} \tag{8}$$

Moreover, the oil weight will be also considered inside this mass group. The same procedure has been followed, obtaining a final value of :

$$\mathbf{W_{oil} = 18 \ kg} \tag{9}$$

4.4.2 Payload

The weight associated to the payload will mainly include the crew, represented by the pilot and the observer. Since a full load case will be simulated, both weights are considered together with their parachutes. The weight of the pilot/observer-parachute set is estimated as 90 kg and therefore, the total payload weight is :

$$\mathbf{W_{payload}} = W_{pilot+parachute} + W_{observer+parachute} = \mathbf{180 \ kg} \tag{10}$$

4.4.3 Operational Empty Weight (OEW)

OEW is defined as the weight of the aircraft without the fuel and payload, so that is 572 kg. In this group, all elements and parts that comprise the fuselage are included. The estimated weights for each of the components are shown below:

Operational Empty Weight (OEW)	
Element	**Weight [kg]**
Engine	160
Rotor blades	90
Rotor system	50
Pylon structure	51
Pilot seat	3
Co-pilot seat	3
Clutch system	6
Mechanical starter	10
Instruments and equipment	25
Horizontal stabilizer	18
Vertical stabilizer	10
Fuselage structure	30
Main landing gear	56
Tail landing gear	4
Wheels	8
Formers	12
Stringers	12
Engine cowling	12
Plywood+fabric fairing	12
TOTAL	572

Table 3: Empty weight estimation

Once all weights are estimated, equation 6 is fulfilled :

$$W_{MTOW} = W_{OEW} + W_{payload} + W_{fuel+oil} = 572 + 180 + 98 = 850\ kg \tag{11}$$

At this point, it is important to remark several considerations. First of all, the engine weight accounts for the engine system, propeller and its own weight. Besides this, the pylon structure includes several components like the top joint, the pilot control column, pylon struts, among others. Furthermore, the plywood skin and the fabric covered have been considered as a single element.

4.5 Loads

The simplified version of the autogyro C-30 will be simulated in a pull up 3.5g maneuver, in which a vertical lift force is assumed to pull the structure up from the rotor. It must be noticed that all loads will be applied according to the Airworthiness Requirements established by the BCAR and explained in the *Regulatory Framework*. The behaviour of the model will be studied when subjected to two loading cases. In the first case, limit loads will be applied whereas in the second one, the fuselage structure must support ultimate loads. The main differences between them are shown below [19]:

- **Limit loads** : refers to the maximum loads expected in service. No safety factor is applied.
- **Ultimate loads** : defined as the limit loads multiplied by a safety factor.

The loads applied to the model can be divided into three types: loads produced by weight of the components, the engine torque and the lift force. When applying the loads several assumptions have been considered in compliance with the normative:

- Acceleration due to gravity is constant and equal to $g = 9.81\ m/s^2$.
- Safety factor applied for ultimate loads is 1.5.
- Design manoeuvring load factor is $n = 3.5$

4.5.1 Weight loads

Weight loads account for most of the loads applied to the fuselage. In fact, it includes all elements of table 3, the payload, fuel and oil. The downward force of gravity acting on each of the components is estimated as equation 12. Where n is the load factor and m represents the mass (weight).

$$F_g = -n \cdot m \cdot g \tag{12}$$

It must be noted that these loads will be applied either as concentrated loads or as uniformly distributed loads. Furthermore, the fuselage configuration explained in *Section 4.3* will be used in order to know where to apply the loads. For the case of the concentrated loads, they will be applied at a specific node(s). The region where a particular component is located will determine which nodes support the load. Besides this, if a 40 N load has to be applied at four nodes, 10 N will be supported by each of them. In the same way, the distributed loads will be applied in the element(s) that corresponds to the zone where the components are installed. Note that in this case, the load is applied through the length of the corresponding element. For instance, it a load of 20 N has to be applied as an uniform load through an element of 2 m, a load of 10 N/m will be introduced. Two examples of are shown in figures 15 and 16.

Moreover, the rotor blades and the rotor system will be considered as one single mass. Therefore, a single concentrated load simulating both weights will be applied at the apex of the pyramid formed by the four pylon struts. Besides this, formers, stringers, plywood+fabric fairing, and engine cowling will be the only components introduced as uniformly distributed loads.

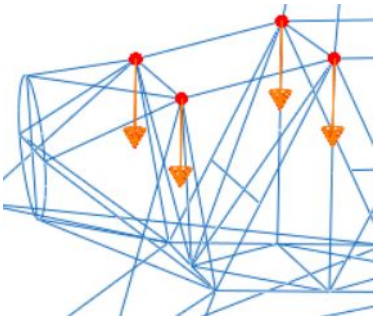

Figure 15: Concentrated load

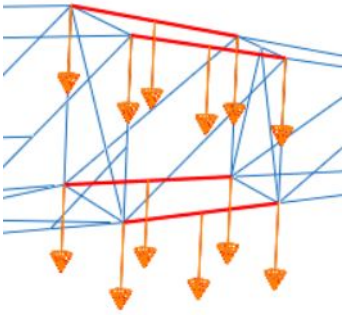

Figure 16: Uniformly distributed load

4.5.2 Lift force

Lift is the aerodynamic force acting perpendicular to the inflow air velocity. As stated previously, the lift generated in an autogyro is produced by the free-spinning rotor. In the simulation, this force is assumed to pull the autogyro up from the rotor. For this reason, the lift will be applied as a vertical concentrated load at the vertex of the pylon structure. In order to estimate the lift equation 13 has been used, where n is the load factor, and $MTOW$ the maximum takeoff weight:

$$L = n \cdot MTOW \cdot g \tag{13}$$

Note that for both weight loads and lift, the safety factor of 1.5 is applied when simulating ultimate loads.

4.5.3 Engine torque

The power unit used in the autogyro C-30 was a Civet I engine of 145 CV (108126 W) at 2140 rpm (maximum continuous power). From the power equation, the torque is estimated as equation 14, where P is the power in Watts and w is the rotational speed in rad/s.

$$T = \frac{P}{w} = 482.5\ Nm \tag{14}$$

The engine torque will be applied to the structure as a concentrated moment at the center of the engine ring, so that is, coincident with the propeller shaft. Besides this, a factor of 1.33 will be applied in order to comply with BCAR standards.

The resultant values of the loads for both cases are shown in tables 4 and 5.

LIMIT LOADS CASE ($n = 3.5g$)			
Element	**Force (N)**	**Element**	**Force (N)**
Pilot	-3090.15	Clutch system	-206.01
Observer	-3090.15	Formers	-412.02
Fuel	-2746.80	Horizontal fin	-618.03
Oil	-618.03	Vertical fin	-343.35
Engine	-5493.60	Fuselage structure	-1030.05
Equipment	-858.38	Stringers	-412.02
Rotor blades	-3090.15	Wheels	-274.68
Rotor system	-1716.75	Mechanical starter	-343.35
Pylon structure	-1751.09	Engine Cowling	-412.02
Pilot seat	-103.01	Plywood+ fabric fairing	-412.02
Observer seat	-103.01	Tail landing gear	-137.34
Landing gear	-1922.76	Lift	29184.75

Table 4: Limit loads

ULTIMATE LOADS CASE ($n = 3.5g$ / SF = 1.5)			
Element	**Force (N)**	**Element**	**Force (N)**
Pilot	-4635.23	Clutch system	-309.02
Observer	-4635.23	Formers	-618.03
Fuel	4120.20	Horizontal fin	-927.05
Oil	-927.05	Vertical fin	-515.03
Engine	-8240.40	Fuselage structure	-1545.08
Equipment	-1287.56	Stringers	-618.03
Rotor blades	-4635.23	Wheels	-412.02
Rotor system	-2575.13	Mechanical starter	-515.03
Pylon structure	-2626.63	Engine Cowling	-618.03
Pilot seat	-154.51	Plywood+ fabric fairing	-618.03
Observer seat	-154.51	Tail landing gear	-206.01
Landing gear	-2884.14	Lift	43777.13

Table 5: Ultimate loads

Figure 17 shows the loaded structure that will be simulated.

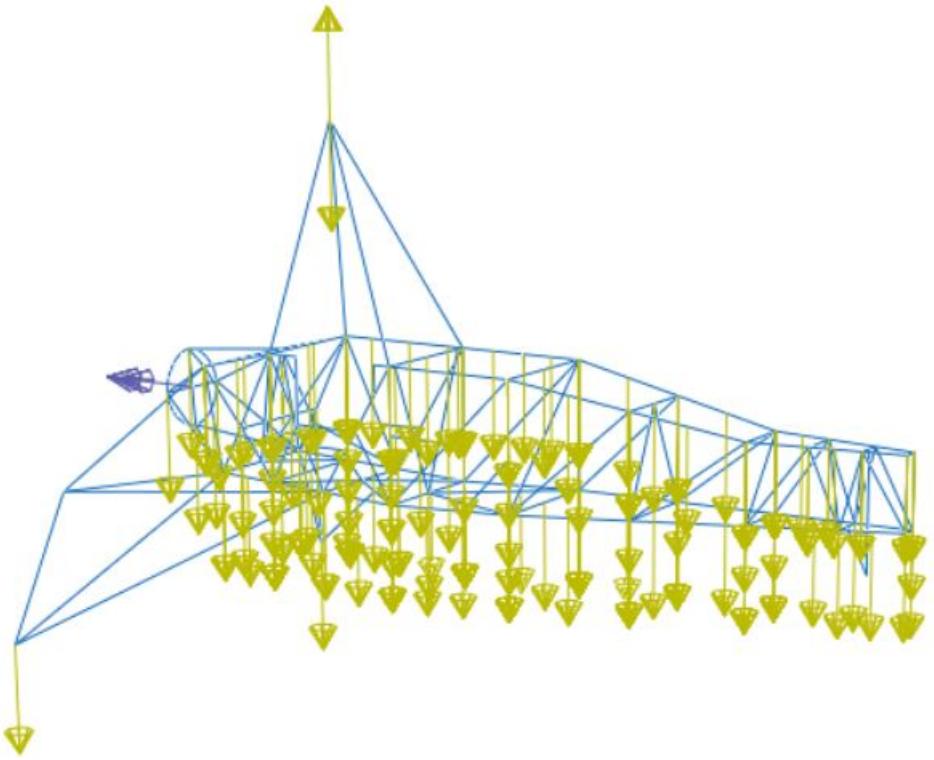

Figure 17: Loads applied to the structure

5 Results

5.1 Structural Stress Analysis

In this section, results for the structural stress analysis are shown. As mentioned previously, the $3.5g$ pull-up maneuver is simulated for two loading cases. Figure 18 depicts the stress distribution results when the system is subjected to limit loads whereas figure 19 shows results for ultimate loads. In both cases, it will be checked if the structure is able to support the loads taking into account the material yield strength ($\sigma_y = 4.35 \cdot 10^8\ Pa$).

In both figures, the beam profiles have been rendered in order to clearly distinguish the stress distribution throughout the fuselage structure. Besides this, since the scope of this paper is the study of the fuselage structure, results regarding the landing gear or pylon structure will not be considered. Stress tensor outputs two different components: an axial stress, and a shear stress caused by shear force and torsion. If one of these values is higher than the maximum allowable stress of the material, a structural failure would be produced. For this reason, results in the legend will depict the maximum value of both (in absolute value) in order to check if the structure deforms plastically in one of the directions. Higher stresses are shown in warm colours while lower ones are in cold colours. All stress values are in pascals (Pa).

Regarding both figures, a very similar behaviour of the structure can be observed. In fact, most stressed zones are found at the beginning of the fuselage, in the first bays. In these zones, the heavier parts are concentrated producing higher stresses. The four principal longerons will be the elements that suffer the most because most concentrated and distributed loads are applied throughout these elements. The larger stresses concentrations are reached in the longerons located in the bottom part of the co-pilot cabin because the most equipment, co-pilot and also the joint with the landing gear is located here. From this point on, the stresses will be progressively reduced when moving to the end of the fuselage. The expected behaviour as there are not many loads in the in the rear part. In fact, only the stabilizers are located. Formers, stringers and fairing are uniformly distributed along these elements but without producing too many stresses.

The maximum stress value achieved for the limit loading case is $1.254{\cdot}10^8\ Pa$ whereas for the ultimate one a value of $1.841 \cdot 10^8\ Pa$ is obtained. In both cases, stresses are well below the material yield strength. The fuselage structure will deform elastically and there will not be plastic deformation. Therefore, it can be stated that the fuselage structure is safe enough to withstand this $3.5g$ pull up maneuver.

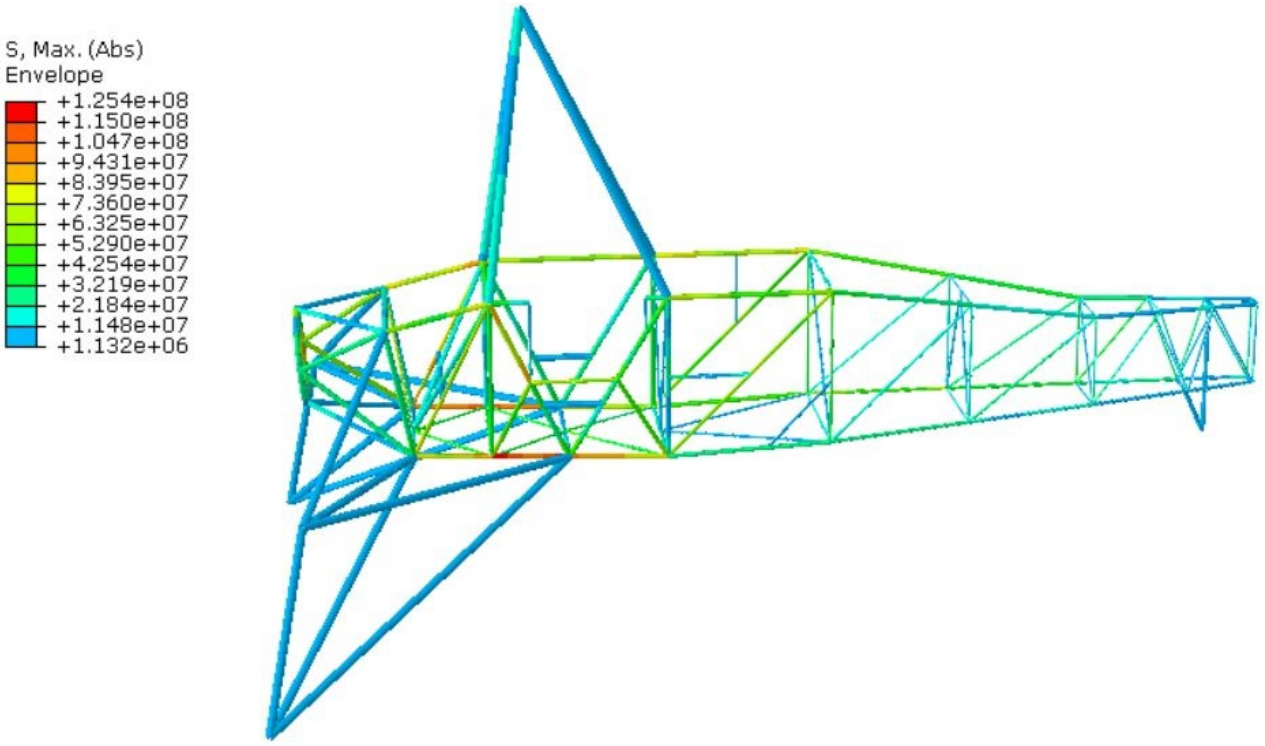

Figure 18: Stress distribution (in Pa) - Limit loads

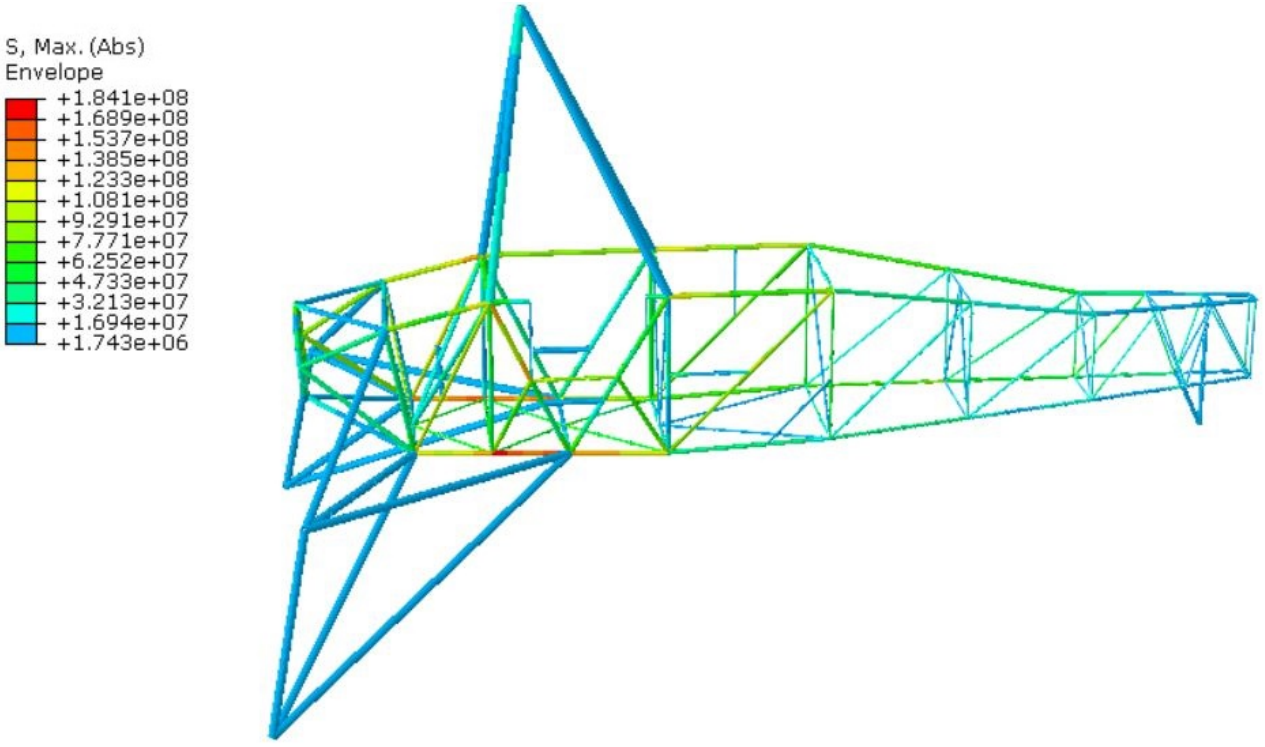

Figure 19: Stress distribution (in Pa) - Ultimate loads

Additionally, the maximum safety factor that can be applied to the structure will be calculated. As it can be observed in previous figures, the maneuver can be performed without problems assuming a safety factor of 1.5. Therefore, considering the same $3.5g$ maneuver, the safety factor will be increased until some of the parts start to deform plastically.

The maximum safety factor that can be used is 5. In fact, when applying this factor to the structure, the first plastic strains are observed in the bottom longerons. As expected, these elements were the most stresses and therefore, the first failures of the structure appear in these zones. This effect can be visualized in figure 20.

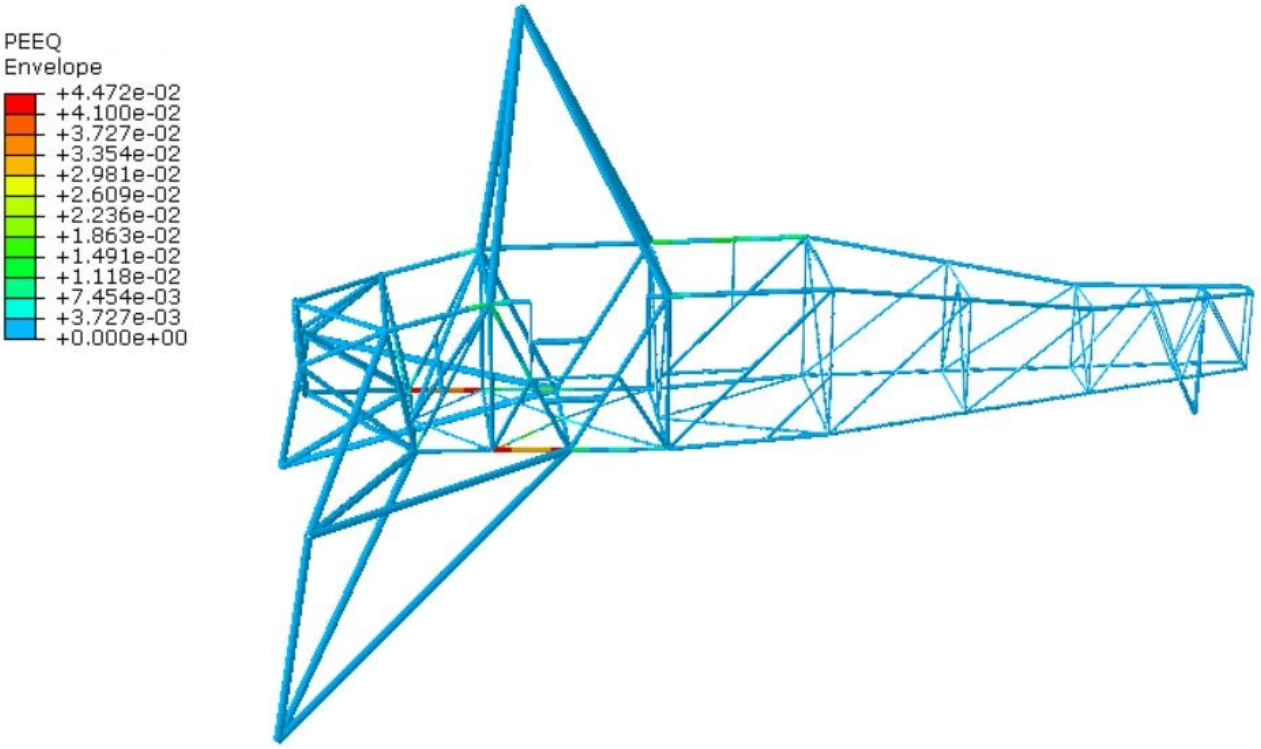

Figure 20: Plastic strain distribution

5.2 Modal Analysis

Finally, a modal analysis has been performed in order to obtain the natural frequencies and mode shapes of the system. The engine and rotor are considered to rotate at 2140 rpm (35.67 Hz) and 200 rpm (3.33 Hz), respectively. For this reason, the frequency range of interest will be set in *Abaqus* between 0 and 40 Hz, and in this way, check if some of the natural frequencies of the structure coincide with the engine or rotor frequency.

In this type of analysis, loads are not applied to the structure. In fact, only boundary conditions are applied. In this case, the autogyro will be pinned from the main and tail landing gear. The reason of not applying loads is mainly because in modal analysis the response of the model to a dynamic excitation is not analyzed. The purpose of the modal analysis is only to determine the natural frequencies and to visualize mode shapes.

In the case of analyzing the response to a dynamic load, a different type of analysis would have to be performed. Generally, this kind of analysis is called frequency or time response analysis, in which the real deformation that an input loading produces on a structure is studied.

Within the frequency range determined, the number of modes obtained is four. Each of the modes corresponds to a certain frequency, as it is depicted in table 6. In this case, neither the engine nor the rotor frequency coincides with the natural frequencies of the structure; therefore it is safe enough. It is important to remark that the natural frequencies can be shifted by re-designing the model since they only depend on the characteristics of the structure (mass and stiffness).

Frequency Analysis	
Mode number	Natural frequency (Hz)
1	16.503
2	18.423
3	23.017
4	37.844

Table 6: Frequencies corresponding to the first modes

Figures 21, 22, 23, and 24 show each of the mode shapes. Note that the legends are not shown because the values of the displacements are not real. In fact, those values are totally arbitrary and have no meaning in modal analysis since there are no loads applied. This type of analysis only serves to visualize the deform shape of the structure but without outputs any real value of the displacements. In this way, the parts that deform the most can be appreciated.

As it can be observed, each of the modes deforms in a specific way. These figures show how the structure will tend to deform at each of these four natural frequencies. In all modes, the rear part of the fuselage is mainly involved. Therefore, if there is a coincidence between the excitation frequency and the natural frequency of the system, a large deformation could be obtained in this specific zone. For this reason, this region should be modified in order to reduce the vibration response.

As mentioned before, the modal analysis is very useful for models that are prepared to work in a dynamic loading environment. When a frequency-dependant load is applied at the natural frequency of the structure, the system may enter in resonance producing large oscillations and displacements. Resonance problems can cause a fracture of the structure. For this reason, modal analysis helps to determine which parts have to be modified in order to avoid potentials problems.

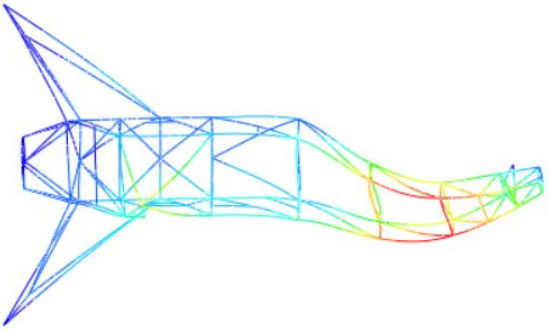

Figure 21: Mode 1

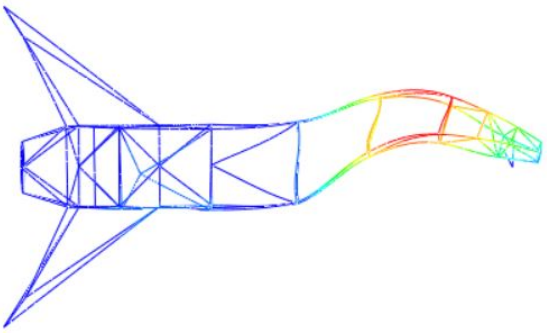

Figure 22: Mode 2

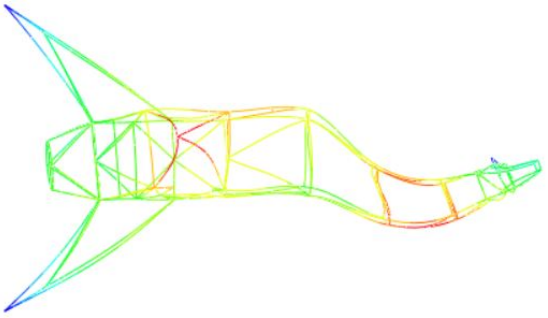

Figure 23: Mode 3

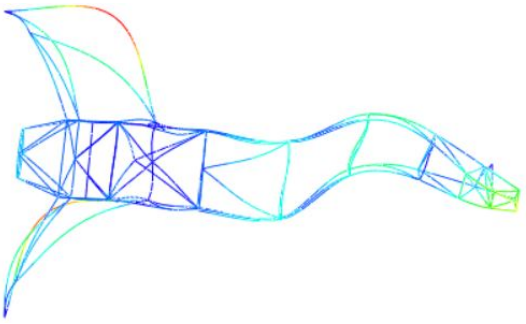

Figure 24: Mode 4

6 Socio-economic impact and project costs

Socio-economic impact

Currently, the main aerial rotorcraft transport is the helicopter, and therefore the design of an autogyro like the C-30 prototype would not have any impact on the society. As stated in the introduction, the ability of the helicopter to hover has become this type of aircraft as one of the most attractive options for companies and governments. The autogyro market is almost ceased compared to the helicopter one. Nevertheless, the impact, if autogyros were produced to the same extent as helicopters are nowadays, will be analysed hereunder.

If military aviation and the government started investing funds in the development and improvement of the autogyro, the era of air transport may change. Nowadays, most modern autogyros have implemented modifications for pre-rotate the rotor, allowing for purely vertical take-off and landing. Moreover, the autogyro can achieve high reliability without the complex rotor system of the helicopter. As a consequence, complexity, maintenance and weight are reduced. Therefore, saving costs and increasing profitability.

Furthermore, since the lift is not produced by a powered rotor, its fuel consumption is lower compared to the helicopter. Therefore, the use of autogyros instead of helicopters would reduce the pollution to the atmosphere. Moreover, it can stay airborne for hours with a greater range and safety, as it cannot stall.

The autogyro could be a good option for different sectors in which flying at low speeds is required and hovering is not needed. In this situation, the autogyro could perform missions at a lower cost and with a higher safety compared to the helicopter. The autogyro could be useful for different sectors oriented to:

- Agriculture: the autogyro can serve to irrigate larger crops.
- Military: reconnaissance and surveillance roles in restricted areas and borders can be performed efficiently due to its great manoeuvrability at low speed.
- Transport: can serve as an effective mean of people and cargo transport with a high payload efficiency.
- Emergency situations: it can help in search and rescue missions or to extinguish fires.

At present, there exist companies that have ongoing projects to improve the performance of the autogyro. However, most autogyro constructions are actually made by amateurs, mainly used for sports exhibition. This is the reason why is almost impossible to know how many autogyros are registered. In fact, depending on the model and characteristics, the prices can range from $7000 to $100,000 [27]. These prices allow people the possibility of flying with a rotary wing aircraft at more affordable prices than buying a helicopter.

Project costs

The budget associated to this thesis can be estimated as:

- **Software**: In order to perform the study, several programs have been used. On the one hand, the *Abaqus Student Version* has been free downloaded; it is free for student and academic uses and hence, the costs is 0 €. Moreover, the *Matlab R2017b student version* has been also used, whose license's price is 70 €.
- **Personnel expenses**: Assuming that the junior annual engineer salary in Spain is about 21000 € [28], the salary per hour stands for 10.17 €. Since the total time devoted to the project has been over 450 hours, personnel expenses can be estimated as 4576.5 €. Note that in this group the salary of the tutor will be included as well. Assuming 30 hours of meetings and an salary per hour of 20 €, the total supervisor cost is 600 €.

Therefore, the total budget of this project stands for 5246.5 €.

Note that more accurate results could be obtained with a full *Abaqus* edition, in which the models are not restricted up to 1000 nodes. However, the cost of this license is about 20000 € per year.

Additionally, the costs associated with the design and manufacturing of the C-30 fuselage structure (skeleton) will be estimated as well. Considering that the mean price of a 4130 Steel tubing is 5.5 € per meter, and that the structure has a tube length of about 60 m, the direct cost associated to the purchase of tubes is 1080 €. Moreover, four operators are required to finish the structure assembled in one month. Therefore, assuming a monthly salary of 1400 € per each operator, the price of the labour cost is 5600 €. Furthermore, an hangar is needed to perform all operations. Renting an autogyro hangar for one month cost is estimated to cost 200 €.

Therefore, the total cost of manufacturing the autogyro C-30 fuselage structure stands for 6880 €.

7 Conclusions and future work

7.1 Conclusions

This project aims to design and analyze a simplified version of the autogyro C-30 fuselage. The autogyro, invented in 1923 by Juan de la Cierva, is still one of the safest aircraft in aviation. Nowadays, there are not many ongoing development projects, due to the growth of the helicopter technology and its advantages over the autogyro. In fact, most people do not very well know what an autogyro is and how it works. And the truth is that without the patents invented by De la Cierva for the autogyro, and implemented years later in the helicopter, this kind of transport could be very different nowadays.

For this reason, in the first part of the project, a little bit of history about rotary-wing aircraft has been introduced. As it has been observed, the contribution of the autogyro to the rotorcraft era was very important. The invention of autogyro became a milestone in aviation history. However, most companies focused on the helicopter development. Nowadays, the autogyro is almost ceased to be marketed and very few research documents can be found about it.

The fuselage structure and the additional elements have been designed in *Abaqus*. This finite element software helps to accurately predict stresses and deformations that appear in a model when subjected to loads. By using this program, the structure can be simulated under different loading conditions without testing the model in real life and therefore, saving money and time. In this case, a pull-up maneuver has been simulated in compliance with the requirements of the BCAR: Section T light gyroplanes. As explained in the *Regulatory framework*, the lack of a proper normative for heavy autogyros has made assume the autogyro C-30 as a light one.

Results have shown that the autogyro C-30 fuselage structure fulfills all strength requirements and that is safe enough to perform a 3.5g pull-up maneuver. The stresses obtained are well below the material yield strength and therefore, the structure will not deform plastically. The larger concentrations of stresses are located in the second bay where the pylon structure and most parts are placed. As expected, the rear part was the one with fewer stresses as there are not many components. Due to the capability of the structure to support a 3.5g pull-up maneuver, the safety was increased until the first plastic deformations were found. A maximum safety factor of 5 can be applied before break. Therefore, it can be stated that the fuselage structure is prepared to support this maneuver.

Besides this, a modal analysis has been performed in which the natural frequencies and modes have been computed. The natural frequencies do not coincide with the normal operating frequency of the rotor and engine, and therefore, it is safe from this point of view. It has been appreciated that the rear part is the zone that would produce larger oscillations in case of enter in resonance. As expected, this zone is less stiffness than the others and therefore, larger displacements are produced.

One possible solution could be to introduce more tubes and in this way, increasing stiffness and mass, producing lower oscillations.

Modal analysis is a very important engineering tool that helps to detect dangerous frequencies that can destroy the structure. It is mainly used in order to determine the modes of the system that may resonate when the input loading frequencies coincide with the natural frequencies of the structure. This will help engineers to determine the potential dangerous modes that have to be avoided in the design.

7.2 Future work

This project can be used as a starting point for future works related to the study of the autogyro C-30. In this way, a better knowledge of this technology can be performed. However, several issues would have to be solved in order to get success. For instance, the development of drawings based on a real autogyro C-30. In this paper, several parts have been estimated as there is no information. Therefore, if it were possible to get into the autogyro C-30 located at the Museo del Aire, complete drawings of the autogyro may be done.

Regarding the fuselage structure, an optimization process can be carried out with the objective of reducing weight, among others. Besides this, with real flight conditions data about different phases of the flight, a different maneuver could be also analysed. Moreover, other parts of the autogyro may be designed and studied. One interesting study could be the design of a landing gear and analysis it during a landing procedure. In the same way, the design and study of the rotor system might help to understand better the autorotation principle.

Furthermore, the use of a full version of *Abaqus*, in which the number of nodes is not restricted to 1000, can produce more precise results. In this paper, the analysis have been performed with a mesh of 993 nodes. The results are quite acceptable but with a finner mesh, results could be even better.

References

[1] Alvi. *Cierva C-30*. Blog. URL: https://alvi3d.blogspot.com/p/vehiculos.html (visited on 10/20/2018).

[2] Maestranza Aérea de Albacete. *Autogiro C-30 MZA - Manual de uso y mantenimiento*. Dec. 1998.

[3] Dr. Robert J. Shaw. *History of flight*. NASA. URL: https://www.grc.nasa.gov/www/k-12/UEET/StudentSite/historyofflight.html (visited on 11/03/2018).

[4] *Leonardo Da Vinci*. The American Institute of Aeronautics and Astronautics (AIAA). URL: https://www.aiaa.org/SecondaryTwoColumn.aspx?id=15129 (visited on 11/03/2018).

[5] J. G. Leishman. *A History of Helicopter Flight*. Cambridge University Press. 2000. URL: https://www.aviatorsdatabase.com/wp-content/uploads/2013/07/A-History-of-Helicopter-Flight-.pdf (visited on 11/07/2018).

[6] P.A. Hufton et al. *General Investigation Into the Characteristics of the C.30 Autogiro*. ARC technical report. H.M. Stationery Office, 1939.

[7] J. G. Leishman. *Principles of Helicopter Aerodynamics*. Second edition. Cambridge aerospace series. Cambridge University Press, 2006, pp. 692–694.

[8] *The Theory of the Autogiro*. All the World's Rotorcraft. URL: http://www.aviastar.org/theory/autogiro/index.html (visited on 11/10/2018).

[9] Anand Saxena. "GYROPLANE - A Technical Essay on the Gyroplane". In: (Nov. 2018). URL: https://www.researchgate.net/publication/265063892_GYROPLANE_-_A_Technical_Essay_on_the_Gyroplane.

[10] The Editors of Encyclopaedia Britannica. "Juan de la Cierva". In: (Dec. 2018). URL: https://www.britannica.com/biography/Juan-de-la-Cierva (visited on 12/10/2019).

[11] C. LL. Bullock. *The Rota Gyroplane: Civet I Aero-Engine*. 1st ed. Air Ministry, UK, 1934.

[12] Aviation Corner website. *C-30*. [Online]. URL: http://www.aviationcorner.net/show_photo_en.asp?id=164966 (visited on 12/12/2019).

[13] C N Colson. *Avro C.30 Direct-Control Autogiro (British)*. NASA. 1934. URL: https://ntrs.nasa.gov/archive/nasa/casi.ntrs.nasa.gov/19930090361.pdf (visited on 12/13/2019).

[14] *Skyworks Global website*. [Online]. URL: https://www.skyworks-global.com/#section-about-skyworks (visited on 12/20/2019).

[15] *The e-Potential of Modern Gyroplanes*. [Online]. URL: http://www.ecolight.ch/Images/e-Gyro.pdf (visited on 12/20/2019).

[16] *EASA website*. [Online]. URL: https://www.easa.europa.eu/the-agency/the-agency (visited on 01/13/2019).

[17] Council of the European Union European Parliament. *Regulation (EC) No 216/2008*. 2008. URL: https://eur-lex.europa.eu/legal-content/EN/ALL/?uri=CELEX:32008R0216 (visited on 01/13/2019).

[18] *Civil Aviation Authority website*. [Online]. URL: https://www.caa.co.uk/home/ (visited on 01/14/2019).

[19] Civil Aviation Authority. *British Civil Airworthiness Requirements: Section T Light Gyroplanes*. Cap Series. Stationery Office, 2013.

[20] D.S. Burnett. *Finite element analysis: from concepts to applications*. Addison-Wesley Pub. Co., 1987.

[21] *FEM Projects*. [Online]. URL: http://www.bonitechnologies.com/training/fem-projects/ (visited on 01/18/2019).

[22] C. LL. Bullock. *The Rota Gyroplane: Civet I Aero-Engine*. 1st ed. Vol. 2. Air Ministry, UK, 1934.

[23] USA Industries. *Nominal Tube Dimensions Chart (BWG)*. [Online]. URL: https://www.usaindustries.com/charts-and-tables/birmingham-wire-gauge-bwg-boiler-condenser-tube-size-chart.php (visited on 01/20/2019).

[24] *ASM Aerospace Specification Metals*. [Online]. URL: http://asm.matweb.com/search/SpecificMaterial.asp?bassnum=m4130r (visited on 01/20/2019).

[25] C. Niu and M.C.Y. Niu. *Airframe Structural Design: Practical Design Information and Data on Aircraft Structures*. Airframe book series. Adaso Adastra Engineering Center, 1999. Chap. 11.

[26] C. LL. Bullock. *The Rota Gyroplane: Civet I Aero-Engine*. 1st ed. Vol. 1. Air Ministry, UK, 1934.

[27] *Gyroplanes prices*. [Online]. URL: https://www.barnstormers.com/ad_manager/listing.php?main=Experimental&sub=Gyrocopter (visited on 02/07/2019).

[28] *Junior Engineer Salaries in Spain*. [Online]. URL: https://www.glassdoor.com/Salaries/madrid-junior-engineer-salary-SRCH_IL.0,6_IM1030_KO7,22.htm (visited on 02/09/2019).

Appendix A - Fuselage structure dimensions

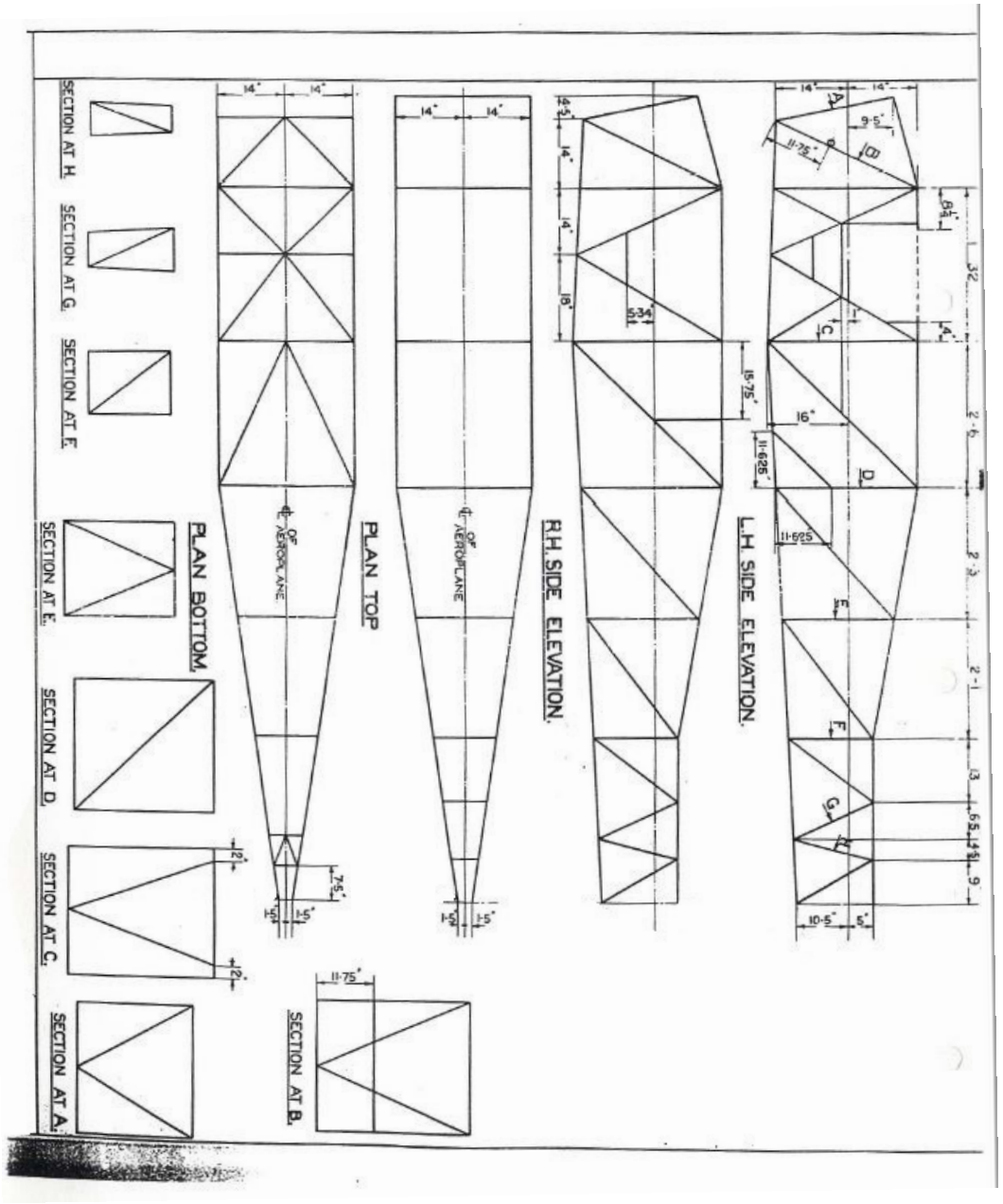

Appendix B - Fuselage tube diagram

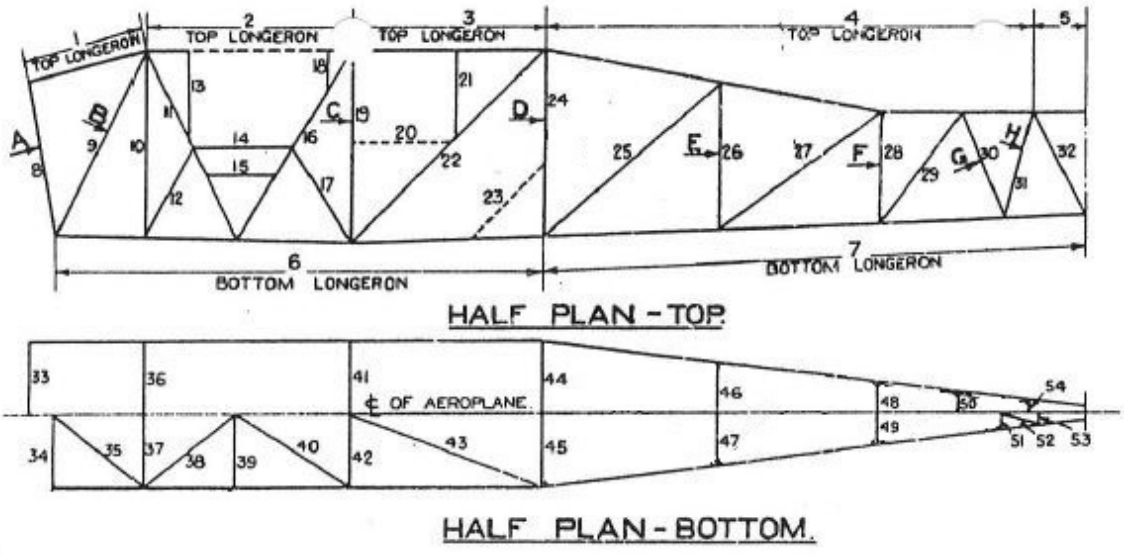

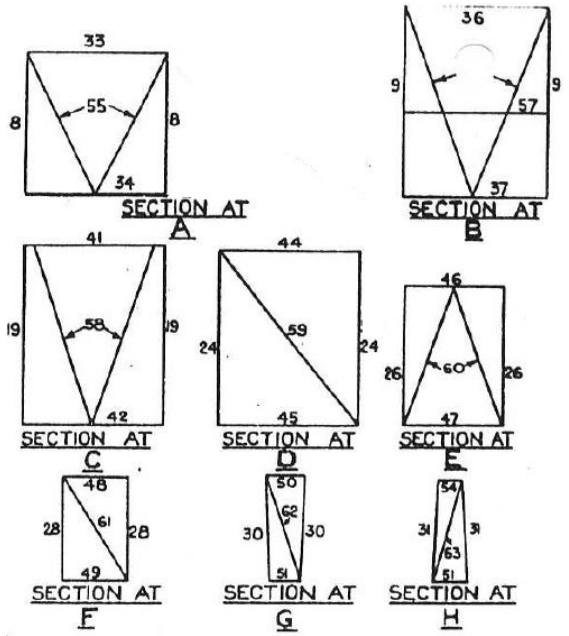

Appendix C - Nominal tubes dimensions

Member Nº	Length (mm)	Outside (mm)	Inside (mm)
1	483.60	25.40	23.62
2	812.80	25.40	23.62
3	762.00	25.40	23.62
4	1950.00	22.23	20.45
5	228.60	22.23	20.45
6	1932.44	22.23	20.45
7	2161.50	19.05	17.63
8	607.72	25.40	23.62
9	795.15	19.05	17.27
10	726.66	22.23	19.28
11	422.49	25.40	22.45
12	390.89	22.23	19.28
13	381.01	15.88	14.45
14	395.52	19.05	16.10
15	274.78	31.75	29.97
16	871.68	25.40	22.45
17	447.51	22.23	19.28
18	164.91	15.88	14.45
19	762.00	22.23	19.28
20	381.00	19.05	17.63
21	355.60	15.88	14.10
22	1077.63	19.05	17.27
23	427.69	15.88	14.45
24	725.56	15.88	14.10
25	915.75	15.88	14.10
26	574.06	15.88	14.45
27	786.56	15.88	14.45
28	433.79	12.70	11.28
29	545.17	12.70	11.28
30	442.08	12.70	11.28
31	425.73	12.70	11.28
32	455.26	12.70	10.92
33	711.20	28.58	25.63
34	711.20	25.40	22.45
35	503.18	15.88	14.45
36	711.20	28.58	26.80
37	711.20	19.05	17.27
38	503.11	15.88	14.45

Table 7 continued from previous page

Member Nº	Length (mm)	Outside (mm)	Inside (mm)
39	355.60	22.23	20.45
40	579.57	15.88	14.45
41	711.20	19.05	17.63
42	711.20	19.05	17.63
43	841.68	15.88	14.45
44	711.20	19.05	17.63
45	711.20	15.88	14.45
46	511.66	12.70	11.28
47	511.66	12.70	11.28
48	326.90	12.70	11.28
49	326.90	12.70	11.28
50	230.82	12.70	11.28
51	182.80	12.70	11.28
52	82.02	12.70	11.28
53	82.02	12.70	11.28
54	149.54	22.23	19.28
55	704.11	15.88	14.45
56	711.20	15.88	14.45
57	871.04	25.40	22.45
58	820.70	15.88	14.45
59	1015.99	15.88	14.45
60	628.49	15.88	14.45
61	543.17	12.70	11.28
62	487.48	12.70	11.28
63	456.71	12.70	11.28
Main Landing gear		38.30	29.65
Pylon structure		44.00	22.01
Tail Landing gear		28.00	18.75